

Relaxation dynamics in strained fiber bundles

Srutarshi Pradhan* and Per C. Hemmer†

Department of Physics, Norwegian University of Science and Technology, N-7491 Trondheim, Norway

(Received 26 January 2007; revised manuscript received 20 March 2007; published 21 May 2007)

Under an applied external load the global load-sharing fiber bundle model, with individual fiber strength thresholds sampled randomly from a probability distribution, will relax to an equilibrium state, or to complete bundle breakdown. The relaxation can be viewed as taking place in a sequence of steps. In the first step all fibers weaker than the applied stress fail. As the total load is redistributed on the surviving fibers, a group of secondary fiber failures occur, etc. For a bundle with a finite number of fibers the process stops after a finite number of steps, t_f . By simulation and theoretical estimates, it is determined how t_f depends upon the stress, the initial load per fiber, both for subcritical and supercritical stress. The two-sided critical divergence is characterized by an exponent $-1/2$, independent of the probability distribution of the fiber thresholds.

DOI: 10.1103/PhysRevE.75.056112

PACS number(s): 62.20.Mk

I. INTRODUCTION

Bundles of fibers, with a statistical distribution of breakdown thresholds for the individual fibers, are simple and interesting models of failure processes in materials. They can be analyzed to an extent that is not possible for most materials (for reviews, see [1–5]).

We consider a bundle with a large number N of elastic and parallel fibers, clamped at both ends. When the load on fiber i is increased beyond a threshold value x_i , the fiber ruptures. The breakdown thresholds x_i for the separate fibers are assumed to be independent random variables with a probability density $p(x)$, and a corresponding cumulative distribution function $P(x)$:

$$\text{Prob}(x_i \leq x) \equiv P(x) = \int_0^x p(y) dy. \quad (1)$$

The mechanism for how the extra stress caused by a fiber failure is redistributed among the unbroken fibers must be specified. We study here the classical version, the equal-load-sharing model, in which a ruptured fiber carries no load, and the increased stress caused by a failed element is shared equally by all the remaining intact fibers in the bundle [6].

If an external load F is applied to a fiber bundle, the resulting failure events can be seen as a sequential process [7–9]. In the first step all fibers that cannot withstand the applied load break. Then the stress is redistributed on the surviving fibers, which compels further fibers to fail, etc. This iterative process continues until all fibers fail, or an equilibrium situation with a nonzero bundle strength is reached. Since the number of fibers is finite, the number of steps, t_f , in this sequential process is *finite*. In this paper we determine how t_f depends upon the number of fibers and, more importantly, upon the stress σ , the applied external load per fiber,

$$\sigma = F/N. \quad (2)$$

At a force x per surviving fiber, the total force on the bundle is x times the number of intact fibers. The expected or average force at this stage is therefore

$$F(x) = Nx[1 - P(x)]. \quad (3)$$

One may consider x to represent the elongation of the bundle, with the elasticity constant set equal to unity. The maximum F_c of $F(x)$ corresponds to the value x_c for which dF/dx vanishes. Thus

$$1 - P(x_c) - x_c p(x_c) = 0. \quad (4)$$

We characterize the state of the bundle as *subcritical* or *supercritical* depending upon the stress value relative to the critical stress

$$\sigma_c = F_c/N, \quad (5)$$

above which the bundle collapses completely. Critical properties of fiber bundles have been discussed before, but with a signature different from the one that we use here, and always with the critical point approached from the subcritical side [3,8,10]. The function $t_f(\sigma)$ that we focus on, however, exhibits critical divergence when the critical point is approached from *either* side. As an example, we show in Fig. 1

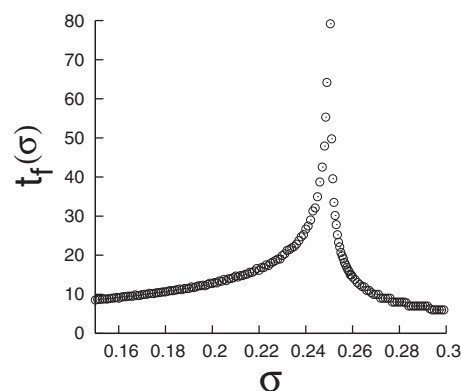


FIG. 1. Number of relaxation steps $t_f(\sigma)$ for a fiber bundle with a uniform threshold distribution (11). Here $\sigma_c = 0.25$. The figure is based on 1000 samples, each with $N = 10^6$ fibers.

*Electronic address: pradhan.srutarshi@ntnu.no

†Electronic address: per.hemmer@ntnu.no

$t_f(\sigma)$ obtained by simulation for a uniform threshold distribution.

We study the stepwise failure process in the bundle, when a fixed external load $F=N\sigma$ is applied. Let N_t be the number of intact fibers at step t , with $N_0=N$. We want to determine how N_t decreases until the degradation process stops. With N_t intact fibers, an expected number

$$[NP(N\sigma/N_t)] \quad (6)$$

of fibers will have thresholds that cannot withstand the load, and consequently these fibers break immediately. Here $[X]$ denotes the largest integer not exceeding X . The number of intact fibers in the next step is therefore

$$N_{t+1} = N - [NP(N\sigma/N_t)]. \quad (7)$$

Since N is a large number, the ratio

$$n_t = \frac{N_t}{N} \quad (8)$$

can for most purposes be considered a continuous variable. By (7) we have essentially [7–9]

$$n_{t+1} = 1 - P(\sigma/n_t). \quad (9)$$

In Sec. II we study $t_f(\sigma)$ in the supercritical domain, while Sec. III is devoted to subcritical situations. Simulation results are presented for two threshold distributions, the uniform and a Weibull distribution, and these are compared with detailed analytic results. The theoretical analysis is, however, not limited to these special threshold distributions. In Sec. IV we summarize our results and discuss briefly the approximations involved.

II. SUPERCRITICAL RELAXATION

We investigate first the supercritical situation, $\sigma > \sigma_c$, with positive values of

$$\epsilon = \sigma - \sigma_c, \quad (10)$$

and start with the simplest model.

A. Uniform threshold distribution

Consider a bundle in which the failure thresholds are distributed according to the uniform distribution

$$P(x) = \begin{cases} x & \text{for } 0 \leq x \leq 1, \\ 0 & \text{for } x > 1. \end{cases} \quad (11)$$

For this case the load curve (3) is parabolic,

$$F = Nx(1-x), \quad (12)$$

with the critical point at $x_c=1/2$, $\sigma_c=1/4$. Simulation results for the uniform threshold distribution are presented in Fig. 1.

The basic equation (9) takes the form

$$n_{t+1} = 1 - \frac{\sigma}{n_t} = 1 - \frac{\frac{1}{4} + \epsilon}{n_t}. \quad (13)$$

This nonlinear iteration can be transformed into a linear one by the following procedure. Introduce first

$$n_t = \frac{1}{2} - y_t \sqrt{\epsilon}, \quad (14)$$

into (13), with a result that may be written

$$\frac{y_{t+1} - y_t}{1 + y_t y_{t+1}} = 2\sqrt{\epsilon}. \quad (15)$$

Setting

$$y_t = \tan v_t, \quad (16)$$

we have

$$2\sqrt{\epsilon} = \frac{\tan v_{t+1} - \tan v_t}{1 + \tan v_{t+1} \tan v_t} = \tan(v_{t+1} - v_t). \quad (17)$$

Hence $v_{t+1} - v_t = \tan^{-1}(2\sqrt{\epsilon})$, with solution

$$v_t = v_0 + t \tan^{-1}(2\sqrt{\epsilon}). \quad (18)$$

In the original variable the solution reads

$$n_t = \frac{1}{2} - \sqrt{\epsilon} \tan\left(\tan^{-1}\left(\frac{\frac{1}{2} - n_0}{\sqrt{\epsilon}}\right) + t \tan^{-1}(2\sqrt{\epsilon})\right) \quad (19)$$

$$= \frac{1}{2} - \sqrt{\epsilon} \tan[-\tan^{-1}(1/2\sqrt{\epsilon}) + t \tan^{-1}(2\sqrt{\epsilon})], \quad (20)$$

where $n_0=1$ has been used.

Equation (13) shows that when n_t obtains a value in the interval $(0, \sigma)$, the next iteration gives complete bundle failure. Taking $n_t=\sigma$ as the penultimate value gives a lower bound, t_f^l , for the number of iterations, while using $n_t=0$ in (20) gives an upper bound t_f^u . Adding unity for the final iteration, (20) gives the bounds

$$t_f^u(\sigma) = 1 + \frac{2 \tan^{-1}(1/2\sqrt{\epsilon})}{\tan^{-1}(2\sqrt{\epsilon})}, \quad (21)$$

and

$$t_f^l(\sigma) = 1 + \frac{\tan^{-1}\left[\left(\frac{1}{4} - \epsilon\right)/\sqrt{\epsilon}\right] + \tan^{-1}(1/2\sqrt{\epsilon})}{\tan^{-1}(2\sqrt{\epsilon})}. \quad (22)$$

It is easy to show that $t_f^u(\sigma) - t_f^l(\sigma) = 1$. In Fig. 2(a) we show that these bounds nicely embrace the simulation results.

Note that both the upper and the lower bound behave as $\epsilon^{-1/2}$ for small ϵ . A rough approximation near the critical point is

$$t_f(\sigma) \approx K_{\text{super}}(\sigma - \sigma_c)^{-1/2} \quad (23)$$

with $K_{\text{super}} = \pi/2$.

B. General threshold distributions

The uniform distribution is amenable to analysis to a degree not shared by other threshold distributions. Therefore we now discuss how to handle other distributions, and we start by a special case, a Weibull distribution of index 5,

$$P(x) = 1 - e^{-x^5}, \quad x \geq 0. \quad (24)$$

The critical parameters for this case are $x_c=5^{-1/5}=0.72478$ and $\sigma_c=(5e)^{-1/5}=0.5933994$. Simulation results for $t_f(\sigma)$

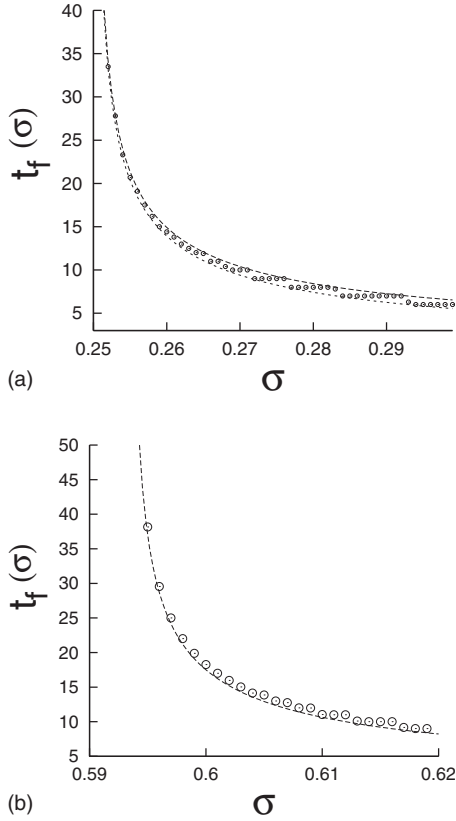


FIG. 2. Simulation results with supercritical stress for (a) the uniform threshold distribution (11), and (b) the Weibull distribution (24). The graphs are based on 10 000 samples with $N=10^6$ fibers in each bundle. Open circles represent simulation data and dashed lines are the theoretical estimates (21) and (22) in (a) and (32) in (b).

are displayed in Fig. 2(b) for the Weibull supercritical case. The variation with the external stress σ is qualitatively similar to the results for the uniform threshold distribution.

The interesting values of the external stress are close to σ_c , because for large supercritical stresses the bundle breaks down almost immediately. For σ slightly above σ_c the iteration function

$$n_{t+1} = f(n_t) = 1 - P(\sigma/n_t) = e^{-(\sigma/n_t)^5}, \quad (25)$$

takes the form sketched in Fig. 3.

The iteration function is almost tangent to the reflection line $n_{t+1}=n_t$ and a long channel of width proportional to ϵ appears. The dominating number of iterations occur within this channel (see Fig. 3). The channel wall formed by the iteration function is almost parabolic and is well approximated by a second-order expression

$$n_{t+1} = n_c + (n_t - n_c) + a(n_t - n_c)^2 + b(\sigma_c - \sigma). \quad (26)$$

Here $n_c = e^{-1/5}$ is the fixed point, $n_{t+1}=n_t$, of the iteration at $\sigma = \sigma_c$. With $u = (n - n_c)/b$ and $\epsilon = \sigma - \sigma_c$ (26) takes the form

$$u_{t+1} - u_t = -Au_t^2 - \epsilon, \quad (27)$$

with $A=ab$. In the channel u changes very slowly, so we may treat the difference equation as a differential equation:

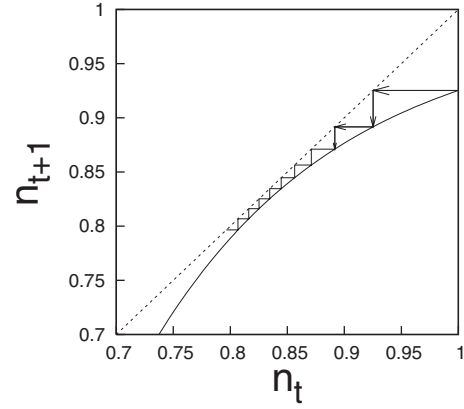


FIG. 3. The iteration function $f(n)$ for the Weibull distribution (24). Here $\sigma=0.6$, slightly greater than the critical value $\sigma_c = 0.593\,399\,4$.

$$\frac{du}{dt} = -Au^2 - \epsilon, \quad (28)$$

with solution

$$t\sqrt{A\epsilon} = -\tan^{-1}(u\sqrt{A/\epsilon}) + \text{constant}. \quad (29)$$

Thus

$$t_e - t_s = (A\epsilon)^{-1/2} [\tan^{-1}(u_s\sqrt{A/\epsilon}) - \tan^{-1}(u_e\sqrt{A/\epsilon})] \quad (30)$$

is the number of iterations *in the channel*, starting with u_s , ending with u_e . This treatment is general and can be applied to any threshold distribution near criticality. Although the vast majority of the iterations occur in the channel, there are a few iterations at the entrance and at the exit of the channel that may require attention in special cases. The situation is similar to type I intermittency in dynamical systems [11], but in our case the channel is traversed merely once.

For the Weibull distribution the expansion (26) has the precise form

$$n_t = e^{-(\sigma/n)^5} \approx e^{-1/5} + (n - n_c) - \frac{5}{2}e^{1/5}(n - n_c)^2 - 5^{1/5}(\sigma - \sigma_c), \quad (31)$$

where $n_c = e^{-1/5}$, $a = \frac{5}{2}e^{1/5}$, $b = 5^{1/5}$, and $A = \frac{5}{2}(5e)^{1/5}$. For completeness we must also consider the number of iteration to reach the entrance to the channel. It is not meaningful to use the quadratic approximation (31) where it is not monotonously increasing, i.e., for $n > n_m = n_c + 1/(2a) = \frac{6}{5}e^{-1/5} \approx 0.98$. Thus we take $n_s = n_m$ as the entrance to the channel, and add one extra iteration to arrive from $n_0=1$ to the channel entrance. [Numerical evidence for this extra step: For $\sigma = \sigma_c$ the iteration (25) starts as follows: $n_0=1.00$, $n_1=0.93$, $n_2=0.90$, while using the quadratic function with $n_0=n_m=0.98$ as the initial value, we get after one step $n_1=0.90$, approximately the same value that the exact iteration reaches after two steps.] With $n_e=0$ we obtain from (30) in the Weibull case the estimate

$$t_f = 1 + (A\epsilon)^{-1/2} [\tan^{-1}(e^{-1/5}\sqrt{A/\epsilon/5b}) + \tan^{-1}(e^{-1/5}\sqrt{A/\epsilon/b})], \quad (32)$$

with $A = \frac{5}{2}(5e)^{1/5}$ and $b = 5^{1/5}$.

We see in Fig. 2(b) that the theoretical estimate (32) gives an excellent representation of the simulation data. Near the critical point (32) has the asymptotic form

$$t_f \approx \pi(A\epsilon)^{-1/2} = K_{\text{super}}(\sigma - \sigma_c)^{-1/2}, \quad (33)$$

with $K_{\text{super}} = \pi(2/5)^{1/2}(5e)^{-1/10}$. The critical index is the same as for the uniform threshold distribution. The divergence is caused by the large number of iterations in the narrow channel in Fig. 3. For a general threshold distribution such a channel will always be present, and therefore the divergence (33) is universal. Moreover, the amplitude of $(\sigma - \sigma_c)^{-1/2}$, as well as an excellent representation of the complete $t_f(\sigma)$ function may, for a given threshold distribution, be obtained by the same procedure as used above for the Weibull case.

III. SUBCRITICAL RELAXATION

We now assume the external stress to be subcritical, $\sigma < \sigma_c$, and introduce the positive parameter

$$\epsilon = \sigma_c - \sigma \quad (34)$$

to characterize the deviation from the critical point.

Also in the subcritical situation a bundle with the uniform threshold distribution (11) can be analyzed analytically to a greater extent than for other distributions, and consequently we start with this case.

A. Uniform threshold distribution

Using a similar method as in the supercritical situation we introduce into (13),

$$n_t = \frac{1}{2} + \sqrt{\epsilon}/z_t, \quad (35)$$

as well as $\sigma = \frac{1}{4} - \epsilon$, with the result

$$2\sqrt{\epsilon} = \frac{z_{t+1} - z_t}{1 - z_{t+1}z_t}. \quad (36)$$

In this case

$$z_t = \tanh w_t \quad (37)$$

is the useful substitution. It gives

$$2\sqrt{\epsilon} = \frac{\tanh w_{t+1} - \tanh w_t}{1 - \tanh w_{t+1} \tanh w_t} = \tanh(w_{t+1} - w_t). \quad (38)$$

Thus $w_{t+1} - w_t = \tanh^{-1}(2\sqrt{\epsilon})$, i.e.,

$$w_t = w_0 + t \tanh^{-1}(2\sqrt{\epsilon}). \quad (39)$$

Starting with $n_0 = 1$, we obtain $z_0 = 2\sqrt{\epsilon}$ and hence

$$w_t = (1+t)\tanh^{-1}(2\sqrt{\epsilon}). \quad (40)$$

This corresponds to

$$n_t = \frac{1}{2} + \frac{\sqrt{\epsilon}}{\tanh[(1+t)\tanh^{-1}(2\sqrt{\epsilon})]} \quad (41)$$

in the original variable.

Apparently n_t reaches a fixed point $n^* = \frac{1}{2} + \sqrt{\epsilon}$ after an infinite number of iterations. However, our bundle contains a finite number of fibers, and therefore only a finite number of steps is needed for the iteration to arrive at a fixed point N^* of the integer iteration (7),

$$N_{t+1} = N - (\sigma N^2/N_t). \quad (42)$$

Since $X \leq [X] < X+1$ a fixed point N^* of (42) must satisfy [8]

$$\frac{N}{2}(1 + \sqrt{1-4\sigma}) \leq N^* < \frac{1}{2}[N+1 + \sqrt{N^2(1-4\sigma) + 2N+1}]. \quad (43)$$

It is interesting to note that (42) has in general several fixed points for a given value of σ . With $N=10^6$ and $\sigma=0.249$, for instance, there are nine fixed points, viz. 531 623, 531 624, ..., 531 631, the complete set of integers within the interval (43). Since our iteration starts high at $N_0=N$, with steadily decreasing values of N_t , it will stop at the upper fixed point, the largest integer satisfying (43).

As long as $N(1-4\sigma) \gg 1$, which is fulfilled in our simulations, we may take

$$N_u^* = \frac{N}{2}(1 - \sqrt{1-4\sigma}) + \frac{1}{2}[1 + (1-4\sigma)^{-1/2}] \quad (44)$$

as a good approximation to the upper fixed point [in the example above (44) gives 531 631.1, compared with $N_u^* = 531 631$].

As a consequence we use

$$n_t = \frac{N_u^*}{N} = \frac{1}{2} + \sqrt{\epsilon} + \frac{1}{4N}(2 + \epsilon^{-1/2}) \quad (45)$$

as the final value in (41). Consequently we obtain the following estimate for the number of iterations to reach this value:

$$t_f(\sigma) = -1 + \frac{\coth^{-1}[1 + (1 + 2\sqrt{\epsilon})/4N\epsilon]}{\tanh^{-1}(2\sqrt{\epsilon})}. \quad (46)$$

We see in Fig. 4(a) that the simulation data are well approximated by the analytic formula (46).

For very large N (46) is approximated by

$$t_f = \frac{\ln(N)}{4} \epsilon^{-1/2} = K_{\text{sub}}(\sigma_c - \sigma)^{-1/2} \quad (47)$$

with $K_{\text{sub}} = \ln(N)/4$. The critical behavior is again characterized by a square root divergence.

B. General threshold distribution

Again we use the Weibull distribution (24) as an example threshold distribution. Simulation results for the subcritical Weibull distribution are shown in Fig. 4(b).

Forgetting for the moment the finiteness of the fiber bundle, the iteration (9),

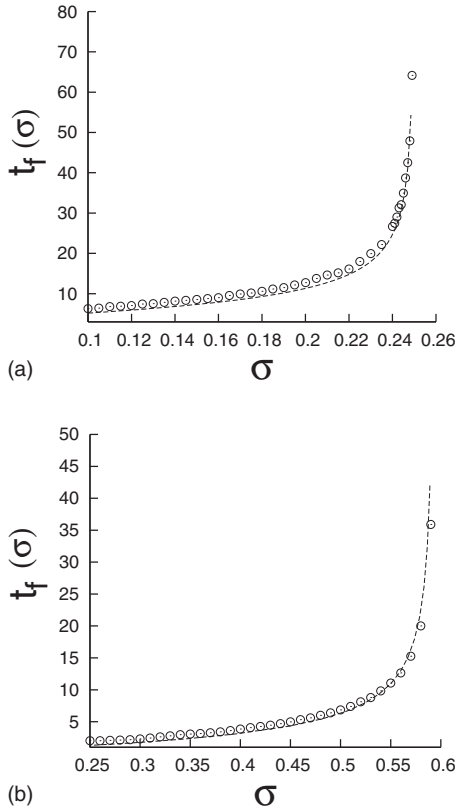


FIG. 4. Simulation results with subcritical stress for (a) the uniform threshold distribution, and (b) the Weibull distribution (24). The graphs are based on 10 000 samples with $N=10^6$ fibers in each bundle. Open circles represent simulation data and the dotted lines are the theoretical estimates, Eq. (46) in (a) and Eqs. (56) and (57) in (b).

$$n_{t+1} = 1 - P(\sigma/n_t), \quad (48)$$

will reach a fixed point n^* after infinite many steps. The deviation from the fixed point, $n_t - n^*$, will decrease exponentially near the fixed point, [7–9, 12]

$$n_t - n^* \propto e^{-t/\tau}, \quad (49)$$

with

$$\tau = 1/\ln[n^{*2}\sigma^{-1}/p(\sigma/n^*)]. \quad (50)$$

For the Weibull threshold distribution, in particular,

$$p(\sigma/n^*) = 5(\sigma/n^*)^4 \exp[-(\sigma/n^*)^5] = 5\sigma^4/n^{*3}, \quad (51)$$

and thus

$$\tau = 1/\ln(n^{*5}/5\sigma^5) \quad (52)$$

for the Weibull case. If we allow ourselves to use the exponential formula (49) all the way from $n_0=1$, we obtain

$$n_t - n^* = (1 - n^*)e^{-t/\tau}. \quad (53)$$

For a finite number N of fibers the iteration will stop after a finite number of steps. It is a reasonable supposition to assume that the iteration stops when $N_t - N^*$ is of the order 1.

This corresponds to take the left-hand side of (53) equal to $1/N$. The corresponding number of iterations is then given by

$$t_f = \tau \ln[N(1 - n^*)] \quad (54)$$

in general, and

$$t_f = \frac{\ln[N(1 - n^*)]}{\ln(n^{*5}/5\sigma^5)} \quad (55)$$

in the Weibull case. Solving the Weibull iteration $n^* = \exp[-(\sigma/n^*)^5]$ with respect to σ and inserting into (55), we obtain

$$t_f = -\frac{\ln[N(1 - n^*)]}{\ln[5(-\ln n^*)]}, \quad (56)$$

$$\sigma = n^*(-\ln n^*)^{1/5}. \quad (57)$$

These two equations represent the function $t(\sigma)$ on parameter form, with n^* running from $n_c = e^{-1/5}$ to $n^* = 1$. In Fig. 4(b) this theoretical estimate is compared with the simulation data. The agreement is satisfactory.

For $n^* = n_c = e^{-1/5}$ (56) shows that t_f is infinite, as it should be. To investigate the critical neighborhood we set $n^* = n_c(1 + \xi)$ with ξ small, to obtain to lowest order

$$t_f = \frac{\ln(N)}{5\xi}, \quad (58)$$

$$\sigma_c - \sigma = \frac{5}{2}\sigma\xi^2. \quad (59)$$

The combination of (58) and (59) gives, once more, the square root divergence

$$t_f(\sigma) \simeq K_{\text{sub}}(\sigma_c - \sigma)^{-1/2}, \quad (60)$$

now with the magnitude

$$K_{\text{sub}} = 10^{-1/2}(5e)^{-1/10} \ln(N). \quad (61)$$

For a general threshold distribution the divergence and its amplitude are most easily deduced by expanding both the load curve $\sigma = x[1 - P(x)]$ and the characteristic time τ around the critical threshold x_c . To lowest contributing order in $x_c - x$ we find

$$\sigma = \sigma_c - \frac{1}{2}[2p(x_c) + x_c p'(x_c)](x_c - x)^2 \quad (62)$$

and

$$\tau = \frac{x_c p(x_c)}{2p(x_c) + x_c^2 p'(x_c)}(x_c - x). \quad (63)$$

Inserting for $(x_c - x)$ from the equation above, and using (55), we find

$$t_f = K_{\text{sub}} \epsilon^{-1/2} \quad (64)$$

with

$$K_{\text{sub}} = x_c p(x_c)[4p(x_c) + 2x_c p'(x_c)]^{-1/2} \ln(N). \quad (65)$$

As a check, the amplitude expression (65) yields the expressions for the uniform and the Weibull distributions derived above.

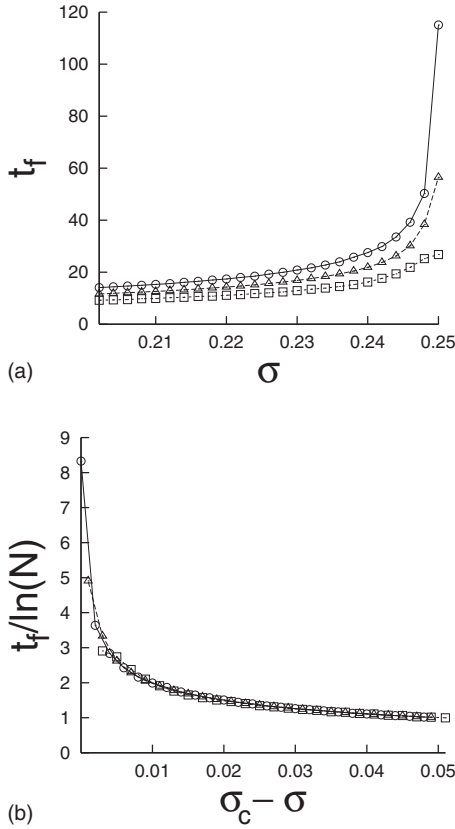


FIG. 5. Numerical evidence for the $\ln(N)$ dependence of t_f in the subcritical case. (a) shows t_f versus σ for different system sizes: 10^6 (circle), 10^5 (triangle), and 10^4 (square). The corresponding data collapse is shown in (b). The data are for the uniform threshold distribution.

To throw some light on how the magnitude of the amplitude K_{sub} depends on the form of the threshold distribution, we consider a Weibull distribution,

$$P(x) = 1 - e^{-(x/a)^k} \quad (66)$$

with varying coefficient k , and constant average strength. With $a = \Gamma(1 + 1/k)$ the average strength $\langle x \rangle$ equals unity, and the width takes the value

$$w = (\langle x^2 \rangle - \langle x \rangle^2)^{1/2} = [\Gamma(1 + 2/k)/\Gamma^2(1 + 1/k) - 1]^{1/2}. \quad (67)$$

Here Γ is the gamma function. Using the power series expansion $\Gamma(1+z) = 1 - 0.577z + 0.989z^2 + \dots$ we see how the width decreases with increasing k ,

$$w \approx \frac{1.52}{k}. \quad (68)$$

For the Weibull distribution (66) we use (65) to calculate the amplitude K_{sub} , with the result

$$K_{\text{sub}} = [\Gamma(1 + 1/k)/2k]^{1/2} (ke)^{-1/2k} \ln(N) \approx (2k)^{-1/2} \ln(N), \quad (69)$$

the last expression for large k . Comparison between (68) and (69) shows that for narrow distributions

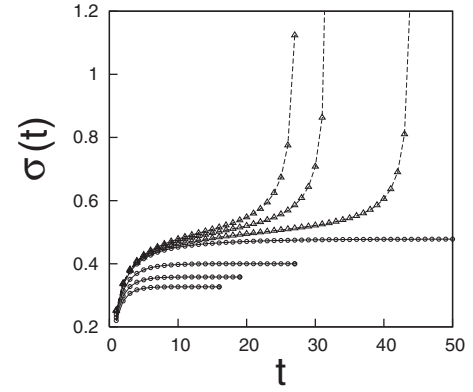


FIG. 6. The evolution of the load per fiber (stress) for the uniform distribution (11). Circles represent data sets for four different applied stresses below the critical stress: $\sigma(0) = 0.22, 0.23, 0.24, 0.25$ and the triangles are the three data sets above critical stress: $\sigma(0) = 0.251, 0.252, 0.253$. A bundle with 10^6 fibers is used.

$$K_{\text{sub}} \propto \sqrt{\text{width}}. \quad (70)$$

That narrow distributions give small amplitudes could be expected: Many fibers with strengths of almost the same magnitude will tend to break simultaneously, hence the relaxation process goes quicker.

To use the exponential approach to the fixed point, as we have done, may seem to be doubtful. But the rationale is that for small σ the starting point $n_0 = 1$ is already rather close to the fixed point, while for larger σ it does not matter much if the first few iterations are not described well by the exponential formula, since in any case the majority of the iterations occur close to the fixed point.

IV. CONCLUDING REMARKS

A detailed numerical and analytic study of the relaxation dynamics in finite fiber bundles subjected to external loads is presented. The relaxation takes place in a number, $t_f(\sigma)$, of steps: In each step all fibers weaker than the load per surviving fiber burst, and the relaxation proceeds until equilibrium is reached or until all fibers have failed. The analytic estimates are based on the average strength of a group of fibers. The comparison with the simulation data using the probabilistic distribution of fiber strength shows that this is a satisfactory calculation procedure.

As a function of the initial stress σ the number of steps, $t_f(\sigma)$, shows a divergence $|\sigma - \sigma_c|^{-1/2}$ at the critical point, both on the subcritical and supercritical side. This is a generic result, valid for a general probability distribution of the individual fiber breakdown thresholds.

On the supercritical side $t_f(\sigma)$ is independent of the system size N for large N . On the subcritical side there is, however, a weak (logarithmic) N dependence, as witnessed by Eqs. (46), (47), and (55). In Fig. 5 we give numerical evidence for this finite-size dependence. We also note that the critical amplitude ratio takes the same value

$$K_{\text{sub}}/K_{\text{super}} = \ln(N)/2\pi \quad (71)$$

for the uniform and the Weibull distributions. This indicates strongly a universal critical amplitude ratio, independent of the threshold distribution.

The effective stress on the bundle shows different behavior for the subcritical and supercritical cases. This has been illustrated in Fig. 6. On the subcritical side the effective stress level finally saturates to a value lower than its critical value. On the other hand for the supercritical cases it grows very quickly showing a diverging tendency.

As a final remark we note that creep phenomena, time-dependent degradation of materials under constant applied load, have been much studied, also in fiber bundle models [13–18]. In the investigations that are closest to our work, equal-load-sharing bundles with viscoelastic fibers are considered [13,14]. In that model instantaneous rupture is prevented through introduction of an explicit damping mechanism for the strain. Although the relaxation mechanism is different from the one in our present study, there are similarities: (i) Criticality is defined by the same static condition (4) as here, (ii) for supercritical loads an equilibrium is reached, while there is a finite lifetime t_f in the supercritical situation, (iii) the lifetime has, to dominating order, no size dependence, and (iv) the lifetime has the same critical divergence $t_f \propto (\sigma - \sigma_c)^{-1/2}$ as in our case. In both cases the critical

exponent value $-\frac{1}{2}$ can be tracked down to the parabolic maximum of the static load curve near criticality. As far as we know, the time to reach equilibrium in the subcritical situation, i.e., the time at which the last fiber breaks, has not yet been given for the viscoelastic model. However, since the characteristic time scale for the infinite viscoelastic bundle diverges with exponent $-1/2$ near criticality [15], the same critical divergence will be seen in both models. The situation is similar for the subcritical finite size dependence of t_f . Apparently, this is not considered in the papers on creep, but we expect that the exponential time dependence towards equilibrium for the infinite bundle would also produce a $\ln(N)$ dependence for this equilibration time for a finite bundle of viscoelastic fibers.

ACKNOWLEDGMENTS

The authors thank B. K. Chakrabarti for useful comments. One of the authors (S.P.) thanks the Research Council of Norway (NFR) for financial support through Grant No. 177958/V30.

-
- [1] *Statistical Models for the Fracture of Disordered Media*, edited by H. J. Herrmann and S. Roux (Elsevier, Amsterdam, 1990).
 - [2] B. K. Chakrabarti and L. G. Benguigui, *Statistical Physics of Fracture and Breakdown in Disordered Systems* (Oxford University Press, Oxford, 1997).
 - [3] D. Sornette, *Critical Phenomena in Natural Sciences* (Springer-Verlag, Berlin, 2000).
 - [4] M. Sahimi, *Heterogenous Materials II: Nonlinear and Breakdown Properties* (Springer-Verlag, New York, 2003).
 - [5] *Modelling Critical and Catastrophic Phenomena in Geoscience*, edited by P. Bhattacharyya and B. K. Chakrabarti (Springer-Verlag, Berlin, 2006).
 - [6] F. T. Peirce, *J. Text. Inst.* **17**, T355 (1926); H. E. Daniels, *Proc. R. Soc. London, Ser. A* **183**, 405 (1945).
 - [7] S. Pradhan and B. K. Chakrabarti, *Phys. Rev. E* **65**, 016113 (2001).
 - [8] S. Pradhan, P. Bhattacharyya, and B. K. Chakrabarti, *Phys. Rev. E* **66**, 016116 (2002).
 - [9] P. Bhattacharyya, S. Pradhan, and B. K. Chakrabarti, *Phys. Rev. E* **67**, 046122 (2003).
 - [10] A. Hansen and P. C. Hemmer, *Trends Stat. Phys.* **1**, 213 (1994).
 - [11] Y. Pomeau and P. Manneville, *Commun. Math. Phys.* **74**, 189 (1980); J. E. Hirsch, B. A. Huberman, and D. J. Scalapino, *Phys. Rev. A* **25**, 519 (1982).
 - [12] See P. C. Hemmer, A. Hansen, and S. Pradhan, “Rupture processes in fibre bundle models,” in *Modelling Critical and Catastrophic Phenomena in Geoscience*, edited by P. Bhattacharyya and B. K. Chakrabarti (Springer-Verlag, Berlin, 2006), pp. 26–55.
 - [13] R. C. Hidalgo, F. Kun, and H. J. Herrmann, *Phys. Rev. E* **65**, 032502 (2002).
 - [14] F. Kun, R. C. Hidalgo, H. J. Herrmann, and K. F. Pal, *Phys. Rev. E* **67**, 061802 (2003).
 - [15] F. Kun, Y. Moreno, R. C. Hidalgo, and H. J. Herrmann, *Europhys. Lett.* **63**, 347 (2003).
 - [16] H. Nechad, A. Helmstetter, R. El Guerjouma, and D. Sornette, *Phys. Rev. Lett.* **94**, 045501 (2005).
 - [17] A. Saichev and D. Sornette, *Phys. Rev. E* **71**, 016608 (2005).
 - [18] H. Nechad, A. Helmstetter, R. El Guerjouma, and D. Sornette, *J. Mech. Phys. Solids* **53**, 1099 (2005).